**Program Digest, 2019 IEEE International Ultrasonics Symposium (IUS)**
**Glasgow, Scotland, October 6-9, 2019**

# Combination of direct, half-skip and full-skip TFM to characterize defect（II）

Xiaoli Han
Institute of Acoustics,
Chinese Academy of Sciences
Beijing, China
hanxiaoli@mail.ioa.ac.cn

Wentao Wu
Institute of Acoustics,
Chinese Academy of Sciences
Beijing, China
wuwentao@mail.ioa.ac.cn

Di Zhang
Institute of Acoustics,
Chinese Academy of Sciences
Beijing, China
d.zhang@mail.ioa.ac.cn

Haitao Wan
Shandong Ruixiang Mould co., LTD.
Jining Shandong, China
13583708833 @126.com

***Abstract*—To improve the accuracy of defect quantification, especially for those defects with a certain extension length, the ultrasonic echo information returned from different regions of defects is explored and combined. Indications of different defect areas are identified and extracted from three different B-scan images obtained by three total focusing method (TFM) modes. Then the different defect areas are combined in a hybrid TFM image to characterize the defect. Simulation is done for defect with extension in vertical direction to prove the validity of the method. For the experiment, a defect buried in the test block invisibly is characterized to further verify the feasibility of the method. Results show that the hybrid TFM is feasible in determining the extension trend and it can give more information in characterizing defects.**

***Keywords—non-destructive testing, ultrasonic imaging, phased arrays, multi-view TFM, sizing***

## I. INTRODUCTION

Non-destructive testing (NDT) is developing towards quantitative non-destructive evaluation (QNDE)[1]. It is not enough to just find defects. We also need to further understand more specific information of the defect, such as size, shape, orientation, etc., which is also called defect characterization. It helps to evaluate how material, workpieces or a system are injured, and get a better estimate of the risk which the defect poses to them. And then the life cycle of the material, workpiece or system can be estimated to determine what to do with them next, such as to be used, repaired or discarded[1, 2].

There are many ways to characterizing defects. Literature [1, 3] reviewed the methods for quantification of defects in ultrasonic testing. Total focusing method (TFM) is a post-processing method based on the full matrix capture (FMC) data, and it achieves focusing point by point in target area [4, 5]. Relative to common beam-forming algorithms, TFM brings in higher detection sensitivity for small defects and improves the resolution[6], so it has been described as the gold standard[7]. Based on the different transmission and reception paths during ultrasonic transmission, TFM is divided into three categories: direct, half-skip, and full-skip TFM [8]. Depending on whether there is mode conversion between different modes of body wave, TFM can be further subdivided into different modes or views[8, 9] . Literature [10] showed that the combination of different modes of TFM imaging can maximize the information about the size or orientation of the defect. It help effectively reduce the possibility of underestimate or missing detection of the defects.

This paper is a continuation of the literature[10]. It explores the method of imaging the different curved surfaces of large defects or a defect group by combining different TFM views to get more knowledge about defects including the trend or shape. And the method is further validated through experiments.

## II. METHOD

### *A. Muti-view TFM*

Literature [9] analyzed all the possible multi-view TFMs when the longitudinal wave (LW) emitted by the transducer obliquely incident on the detected workpiece through the third medium between the array and the workpiece. When the transducer contact with the surface of the workpiece directly (coupled with a little amount of acoustic couplant), which is the situation considered in this paper, the incident body wave into the workpiece is mainly longitudinal. When the longitudinal wave is obliquely incident on the bottom surface of the workpiece or the surface of the defect, there may be both transverse wave (TW) and LW after reflection[9], as shown in Fig. 1. The full ray path includes the transmit path and the receiving path. A transmit path is a path from a transmitter to the image point, and a receiving path is a path from the image point to the receiver. There are three possible transmit paths namely L, LL, and LS and six possible receiving paths namely L, S, LL, LS, SS, SL.

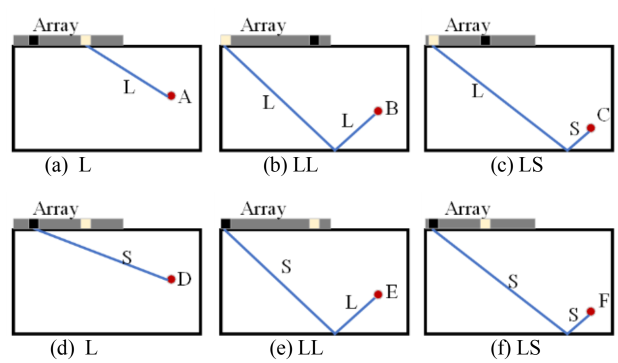


Fig. 1. The possible ray paths when the transducer contacts with the workpiece directly.

National natural science foundation of China (61601454，11604364).

Due to the reciprocity of linear elastodynamics, there are 15unique views out of a total of 18.

For a given view $k$, the TFM intensity $I_k$ at image point $\mathbf{r}$ can be expressed as (1) [9]:

$$I_k(\mathbf{r}) = |\sum_{i,j} a_{ij}(\mathbf{r})\tilde{f}_{ij}\left(\tau_{ij}(\mathbf{r})\right)| \qquad (1)$$

Where： $k$ denotes a certain TFM view or path, $a_{ij}(\mathbf{r})$ is amplitude apodization weight, $\tau_{ij}(\mathbf{r})$ is the time of flight that the ultrasonic wave reaches the current pixel point $\mathbf{r}$ from the $i$th element and then returns to the $j$th element, and $\tilde{f}_{ij}(t)$ represents the analytical signal of the echo trace, which is the Hilbert transform of $f_{ij}(t)$. The main difference in the calculation of each TFM view is $\tau_{ij}(\mathbf{r})$, which is caused by different acoustic propagation paths or wave modes.

When there is a defect group or a defect with a large extension range in the target area, different defects or defect regions may be detected in some different TFM views, while the intensity may be very weak or almost invisible in the other TFM views, as shown in Fig. 2. Three different regions A, B, and C may appear in different TFM views. Region A is most likely shown up in direct TFM view (L-L), region B in half-skip TFM views (LL-L, LS-L, LL-S, LS-S) and region C in full-skip TFM views (LL-LL, LL-SS). That is, different parts of the defect or defect group may be displayed in different TFM views. Therefore, multiple major TFM views can be selected according to the actual situation, and jointly used to evaluate the trend, size or even general shape of the defect or defect group. This is called the combined multi-view TFM. This article will mainly focus on three TFM views with only longitudinal wave mode: direct TFM (L-L), half-skip TFM (LL-L), and full-skip TFM (LL-LL).

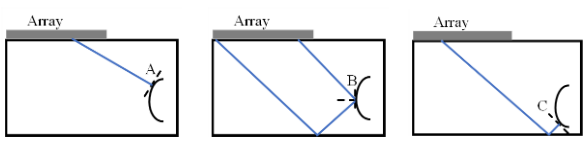

(a) Direct path (b) Half-skip path (c) Full-skip path

Fig.2. Possible paths corresponding to different regions of defect

### *B. The combined multi-view TFM based defect characterization*

The combined multi-view TFM based defect characterization process is as follows:

a) Identify the main TFM paths and views in the inspection. Analyze the main possible ray paths and modes according to the actual situation. It is usually determined by inspection conditions, such as the shape and size of the workpiece, the relative position between the workpiece and the array, and the depth and position that the actual system can scan and reach in the workpiece.

b) The TFM image intensity $I_k$in different views is calculated separately.

First calculate the times of flight in different views, and then calculate the image intensity $I_k$of TFM images according to (1) [9, 10].

c) Defect related indications, artifacts belonging to other views, indications of other interfering signals related to the structure of the workpiece are identified in each current view based on known workpiece shape and structure to identify defect-related imaging regions.

d) The possible defect imaging regions are segmented out to form images $I_k'$ containing only the possible defect regions.

e) Superimpose the images $I_k'$to obtain a combined multi-view TFM image $I$.

$$I = \sum_k I_k' \qquad (2)$$

f) In the combined multi-view TFM image, the defect extension and the possible equivalent size can be determined using a specific defect quantification method[1, 11], such as the dB drops, etc.

## III. Validation

Simulation is done for a defect with extension in vertical direction to prove the validity of the method. For the experiment, a defect buried in the test block invisibly is characterized by the abovementioned combined multi-view TFM based method to further verify the feasibility.

### *A. Simulation*

The medium in the simulation is shown in Fig. 3. It is assumed that there is a spherical defect with a radius of 5 mm in the block. The material is steel, and the defect is filled with water inside. The depth of the steel is 20mm. The transducer parameters are shown in Table I. The simulation is done with Simsonic2D software (SimSonic Suite) to simulate ultrasound propagation and record the FMC echoes based on finite-difference time-domain (FDTD) computations of the elastodynamic equations.

The direct TFM (L-L), half-skip TFM (LL-L), and full-skip TFM (LL-LL) images are showed in Fig.4. The areas marked with red dashed lines are the areas associated with the defect in the three views respectively and artifacts belong to other views are not included.

As shown in Fig. 4(a)~(c), when there are no defects, indications appear in the direct and full-skip images at depths of 20 mm. The echoes at 20 mm are due to the bottom surface of

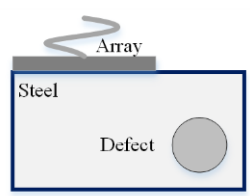

Fig.3. The simulated configuration

TABLE I. PHASED ARRAY PARAMETERS

| Parameter | value |
|---|---|
| ***Element number*** | *32* |
| ***Pitch*** | *0.6 mm* |
| ***Centre frequency*** | *5 MHz* |
| ***Bandwidth (-6 dB)*** | ≥100% |

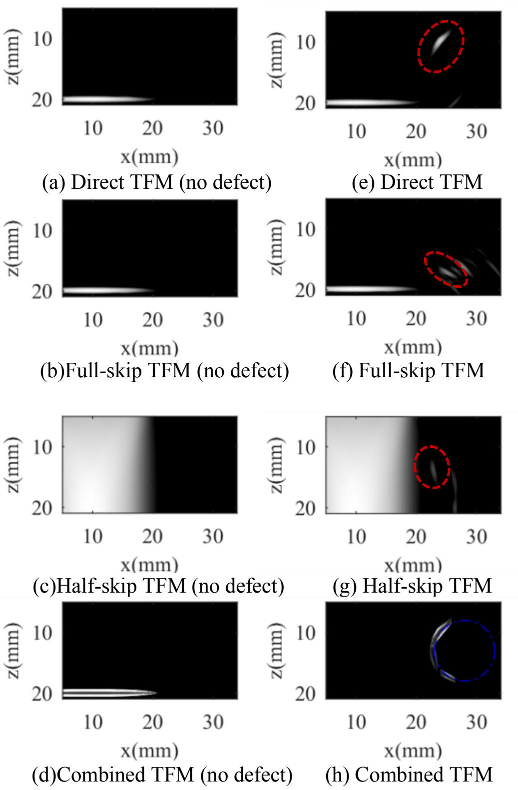


Fig.4 The single mode views and the combined multi-view TFM with and without the spherical defect

the simulated block. As shown in Fig. 4 (e)~(g), after the signal identification in the imaging, the effective signals related to the defect and belonging to the corresponding view are extracted and circled by the red dashed lines. An indication of the defect is displayed in each view. The combined multi-view TFM images with and without defect are obtained using the method described in Section II, as is shown in Fig.4 (d) and Fig.4 (h) . In Fig.4 (d), only the back wall of the block is captured and shown out. The blue dotted and dashed line circled the real position of the defect in Fig.4 (h). It can be seen that after the combination, the extended trend is in good agreement with the actual hemisphere. It is impossible to get the extended trend with a single TFM view.

### *B. Experiment*

The test block is shown in Fig. 5. There are three defects embedded in the test block: a sphere, an ellipsoid, and a cylinder. The radius $r_S$of the sphere is 8 mm. The test block is produced by Shandong Ruixiang Mould co., LTD located Shandong China. Two identical steel plates embedded with half of the volume of the defect  are pressed together by friction welding. At the interface of 20 mm (the plate thickness is 20 mm), most of the sound energy can be transmitted and some will be reflected. This paper take the spherical defect as the target and the array is located at position 3. The parameters of the ultrasonic phased array are shown in Table II. The array parameters are similar to the simulation, but pitch=0.5mm and the relative bandwidth is 80%.  The raw data is collected using USCAS-32 system from Ultrasound Technology Center, Institute of Acoustics, CAS. The system currently supports 32 parallel channels independently

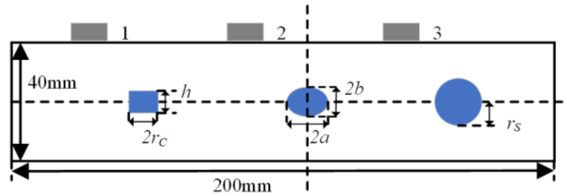


Fig.5 The test block

TABLE II. PHASED ARRAY PARAMETERS

| Parameter | value |
|---|---|
| ***Element number*** | 32 |
| ***Pitch*** | 0.5 mm |
| ***Centre frequency*** | 5 MHz |
| ***Bandwidth (-6 dB)*** | ≥ 60% |

(maximum: 128) and the sampling frequency is 50 MHz.

The three single mode views and the combined multi-view TFM of and the spherical defect is shown in Fig.6, which is compared to the situation when there is no defects. The situation when there is no defects means that the array is placed in a position on the test block where no defects can be scanned.

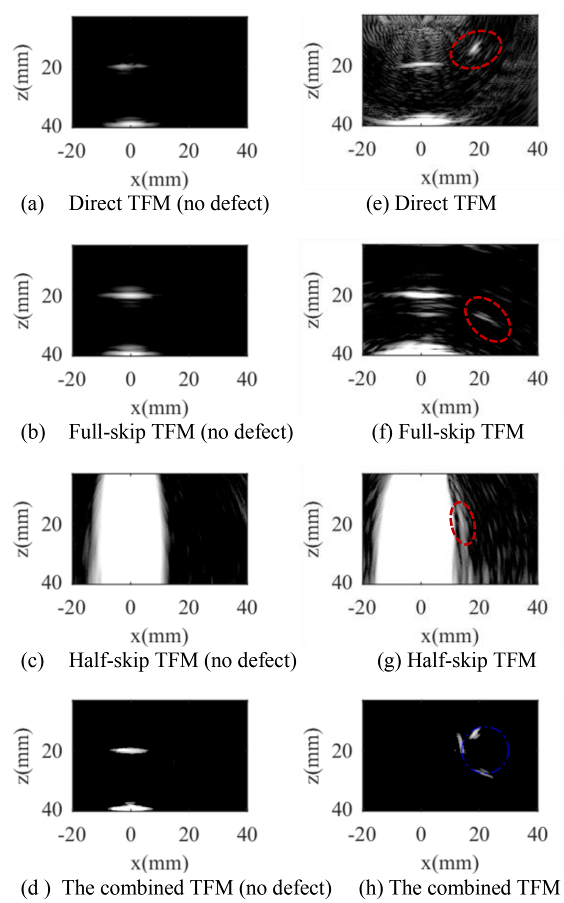


Fig.6 The single mode views and the combined multi-view TFM. In (a)~(d), the defect can not be scanned in any of the view. In (e)~(h) the defect is in the scan area of the array.

As shown in Fig. 6(a)~(b), when there are no defects scaned in the views, indications appear in the direct and full-skip images at depths of 20 mm and 40 mm. The echoes at 40 mm are due to the bottom surface of the test block, and the echo at a depth of 20 mm is related to the processing procedure of the testing block. Acoustic reflection can be produced at the 20 mm interface, which is weak relative to the interface at a depth of 40 mm. As shown in Fig. 6 (e)~(g), after the signal identification in the imaging, the effective signals related to the defect and belonging to the corresponding view are extracted and circled by the red dashed lines.

A combined multi-view TFM image is obtained using the method described in Section II as is shown in Fig.6 (h).The blue dotted and dashed line marks the actual position of the spherical defect according to the array position and image coordinates. It can be seen that after the combination, more defect information is discovered. Judging from the combined result, considering the prior knowledge of the defect, it is consistent with the trend of the circular surface. If the prior knowledge of the defect is not taken into account, at least it can be determined that the defect is a large defect extending in the depth or there is a defect group, with a length of about 15 mm. If a single mode or view of imaging is simply used, the evaluation of the defect can only be underestimated, and the extension of the defect cannot be obtained accurately.

## IV. CONCLUTION

When defect is large or there is a defect group, different modes or views of TFM imaging can image different regions of defect or different defects in the group. In different modes or views, information on different target regions may be captured. Combining different TFM views or modes together, defects can be more comprehensively characterized.

In the experiment, the presence of interference and background noise adds difficulty to the identification of the defect related signs, which is much more complicated than the simulation. There may be artifacts from other views or paths displayed in the current view. To remove the artifacts, all signs must be fully analyzed, and artifacts must be discarded. After the artifacts are discarded, there may be an overlap among the defect area obtained from different views. Fortunately, the positions of the defect areas can be ensured accurately after the sound speed and the time of flight are calibrated, and the overlapping parts will still overlap in the combined image, so it will not cause overestimate.

Although the size of the defect is large in the experiment, this method is still instructive. As long as the defect level is larger than the wavelength, this method has the potential to be applied. Subsequently we will reduce the size of the defect in a new experiment later. In the future, we may try to further determine the surface curvature and even the shape of the defect.

## ACKNOWLEDGMENT

Thanks to the support of the national natural science foundation of China (61601454，11604364).

## REFERENCES

[1] Felice, M.V., and Fan, Z., "Sizing of flaws using ultrasonic bulk wave testing: a review", Ultrasonics, 88（2018）pp. 26-42, 2018.

[2] Achenbach, and J, D., "Quantitative nondestructive evaluation", International Journal of Solids & Structures, 37 (1), pp. 13-27, 2000.

[3] Schmerr, L.W., Jr., Engle, B.J., Sedov, A., and Li, X., "Ultrasonic flaw sizing - An overview", AIP Conference Proceedings, pp.1817-1824, 2013.

[4] Holmes, C., Drinkwater, B.W., and Wilcox, P.D., "Advanced post-processing for scanned ultrasonic arrays: Application to defect detection and classification in non-destructive evaluation", Ultrasonics, 48 (6-7), pp. 636-642, 2008.

[5] Holmes, C., Drinkwater, B.W., and Wilcox, P.D., "Post-processing of the full matrix of ultrasonic transmit–receive array data for non-destructive evaluation", Ndt & E International, 38(8), pp. 701-711, 2005.

[6] Han, X.L., Wu, W.T., Li, P., and Lin, J.: "Application of ultrasonic phased array total focusing method in weld inspection using an inclined wedge". Proc. Piezoelectricity, Acoustic Waves, and Device Applications, SPAWDA Symposium on, Beijing, China, 30 Oct.-2 Nov. 2014.

[7] Kai, E.T., . "Evolution of ultrasound beamformers." Ultrasonics Symposium, 1996. Proceedings, IEEE, 1996.

[8] Jie, Z., Drinkwater, B.W., Wilcox, P.D., and Hunter, A.J., "Defect detection using ultrasonic arrays: The multi-mode total focusing method", Ndt & E International, 43(2), pp. 123-133, 2010.

[9] Nicolas Budyn, R.L.T.B., Jie Zhang, Anthony J. Croxford, Paul D. Wilcox, "A model for multi-view ultrasonic array inspection of small two-dimensional defects", DOI 10.1109/TUFFC.2019.2909988, IEEE Transactions on Ultrasonics, Ferroelectrics, and Frequency Control.

[10] Han, X.L., Wu, W.T., Li, P., and Lin, J.: "Combination of direct, half-skip and full-skip TFM to characterize multi-faceted crack". Proc. Ultrasonics, IEEE Symposium (IUS) 2015, Taipei, China, 2015.

[11] Felice, M.V., Velichko, A., and Wilcox, P.D., "Accurate depth measurement of small surface-breaking cracks using an ultrasonic array post-processing technique", Ndt & E International, 68, pp. 105-112, 2014.